Changes in Hurricanes from a 13-Yr Convection-Permitting Pseudo–Global Warming Simulation

ETHAN D. GUTMANN, ROY M. RASMUSSEN, CHANGHAI LIU, AND KYOKO IKEDA

Research Application Laboratory, National Center for Atmospheric Research, Boulder, Colorado

CINDY L. BRUYERE AND JAMES M. DONE

Mesoscale and Microscale Meteorology Laboratory, National Center for Atmospheric Research, Boulder, Colorado

LUCA GARRÈ, PETER FRIIS-HANSEN, AND VIDYUNMALA VELDORE

DNV GL Climate Action Programme, Group Technology and Research, Oslo, Norway

(Manuscript received 9 June 2017, in final form 24 January 2018)

ABSTRACT

Tropical cyclones have enormous costs to society through both loss of life and damage to infrastructure. There is good reason to believe that such storms will change in the future as a result of changes in the global climate system and that such changes may have important socioeconomic implications. Here a high-resolution regional climate modeling experiment is presented using the Weather Research and Forecasting (WRF) Model to investigate possible changes in tropical cyclones. These simulations were performed for the period 2001–13 using the ERA-Interim product for the boundary conditions, thus enabling a direct comparison between modeled and observed cyclone characteristics. The WRF simulation reproduced 30 of the 32 named storms that entered the model domain during this period. The model simulates the tropical cyclone tracks, storm radii, and translation speeds well, but the maximum wind speeds simulated were less than observed and the minimum central pressures were too large. This experiment is then repeated after imposing a future climate signal by adding changes in temperature, humidity, pressure, and wind speeds derived from phase 5 of the Coupled Model Intercomparison Project (CMIP5). In the current climate, 22 tracks were well simulated with little changes in future track locations. These simulations produced tropical cyclones with faster maximum winds, slower storm translation speeds, lower central pressures, and higher precipitation rates. Importantly, while these signals were statistically significant averaged across all 22 storms studied, changes varied substantially between individual storms. This illustrates the importance of using a large ensemble of storms to understand mean changes.

1. Introduction

Tropical cyclones are a major cause of loss of life and property globally with total economic loss estimates at $36 billion annually since 2000 (Guha-Sapir et al. 2017), and hurricanes are responsible for a large fraction of these damages in North America. Hurricanes are defined as tropical cyclones in the North Atlantic and eastern Pacific Oceans with maximum sustained surface winds greater than $33\,m\,s^{-1}$. The societal impacts are increasing as population increases along tropical-cyclone-prone coasts (Smith and Katz 2013). There is an increasing recognition of the likely impacts of climate change on coastal infrastructure in particular, including the effects of storm surge increases as a result of changes in storm intensities and rising sea levels (Neumann et al. 2015). As a result, any changes in tropical cyclone activity, particularly hurricanes, will have large societal consequences.

Because of the major effect tropical cyclones have on society, much effort has been spent to understand the effect of climate change on tropical cyclone genesis and intensity. Numerous studies have shown that tropical cyclone intensity is linked to warm sea surface temperatures (SSTs) (Emanuel 2007; Hoyos et al. 2006), and there is a strong consensus that SSTs will increase as a result of climate change. As a result, there is reason to suspect that tropical cyclones will become stronger in

Corresponding author: Ethan Gutmann, gutmann@ucar.edu

DOI: 10.1175/JCLI-D-17-0391.1

the future (Mann and Emanuel 2006) and cause more damage (Mendelsohn et al. 2012; Emanuel 2011). However, simple statistical relationships between SSTs and tropical cyclone power dissipation suggest large uncertainty in the future changes; power dissipation may barely increase or it may increase by 300% (Knutson et al. 2010). In addition, increases in atmospheric stability or wind shear could cancel out the thermodynamic effects on intensity (Frank and Ritchie 2001; Tang and Neelin 2004; Swanson 2008).

Changes in tropical cyclone frequency and intensity have been predicted as a result of global climate changes, with numerous studies using both past observations (Emanuel 2005; Mann and Emanuel 2006; Holland and Bruyere 2014; Kossin et al. 2014), numerical simulations of the future (Oouchi et al. 2006; Knutson et al. 2008; Lackmann 2015; Mallard et al. 2013a,b), and theoretical considerations (Emanuel 1987; Holland 1997). Most studies indicate that the number of tropical cyclones will stay the same or decrease slightly (Mallard et al. 2013b). In general, there is more agreement that increasing temperatures will increase tropical cyclone intensity, particularly the more extreme tropical cyclones (categories 3–5 on the Saffir–Simpson scale) (Walsh et al. 2016). However, some studies have suggested that we are approaching thermodynamical limits and that future increases may not be very large (Holland and Bruyere 2014).

Previous work has looked more directly at thermodynamic effects using regional climate models by applying mean changes in temperature and humidity to current weather sequences. For example, Knutson et al. (2008) showed a decrease in the number of hurricanes using an atmospheric model with an 18-km grid when they applied a CMIP3 multimodel ensemble mean change in atmospheric state and SST to a reanalysis weather sequence. When looking at the spread across individual CMIP3 models Knutson et al. (2013) found a significant decrease in tropical storm (wind speeds between 17 and 33 $m\,s^{-1}$) frequency in 5 out of 10 models but a significant increase in the frequency of the most intense hurricanes in 3 out of 10 models (using a 9-km grid). Mallard et al. (2013a,b) performed convection-permitting simulations (6-km grid), but they applied only horizontally constant changes in temperature and humidity to simulations of two months (September of 2005 and 2009) with no changes to the environmental wind field. These studies both covered large domains and focused primarily on cyclone genesis; however, both were limited by either the relatively low resolution of Knutson et al. (2008, 2013) or the short duration and limited change signal applied of Mallard et al. (2013a).

More recent studies used convection-permitting simulations to look at changes in a single hurricane. Lackmann (2015) and Yates et al. (2014) focused on Hurricane Sandy (2012) and performed convection-permitting simulations with the model initialized after Sandy had formed with and without applying a mean change to the background temperature and humidity representative of expected climate change. This approach focuses on the thermodynamic effects on Hurricane Sandy, without complications resulting from variability in genesis. They found decreases in the minimum central pressure (Lackmann 2015) and increase in precipitation (Yates et al. 2014), but no changes in wind speed (Yates et al. 2014). Similarly, Lynn et al. (2009) performed current and future simulations of Hurricane Katrina (2005) using a similar methodology. Lynn et al. (2009) found decreases in the minimum central pressure but also decreases in the mean and maximum wind speeds. Such a decrease in wind speeds seems counter to prevailing expectations (e.g., Knutson et al. 2010) and may simply be a statistical artifact because of the small sample size, a single hurricane. It is possible that future simulations of this particular storm simply shift the track location into a region that is less conducive to faster winds (e.g., over cooler waters or closer to land). Indeed, Lynn et al. (2009) point out that the track does shift toward Florida in their future simulations of Hurricane Katrina. Finally, Hill and Lackmann (2011) studied a larger ensemble of idealized tropical cyclones in a warmer climate. Their ensemble showed a consistent trend toward greater intensities with lower central pressures and higher maximum winds; however, some individual cyclones decreased in intensity, indicating the importance of looking at a larger sample size. This study also left out changes in wind shear, leaving open the possibility that when a more complete set of changes are imposed, hurricane intensity could decrease. Given the variability observed in different studies, it is important to assess a larger ensemble of realistic hurricanes with a more complete set of climate changes imposed on the boundaries.

Our work explores the thermodynamic effects of changes in climate on a collection of hurricane characteristics. We believe it is the first to do so with a long duration (13 yr), continental domain, convection-permitting simulation. It is also the first to do so using a complete set of spatially and temporally variable changes in the relevant climate variables; that is, we modified more variables than temperature and humidity, and the modifications were not constant in time or space. While additional tropical cyclones were simulated in this study, we focus only on hurricanes. A novel aspect of the present study is that most of the simulated hurricanes enter through the boundaries instead of being generated internally or being provided in the initial

conditions. Because of this, we do not examine changes in genesis; however, this approach has the substantial benefit that the hurricanes in current and future climate are initialized almost identically as part of a single continuous model simulation. As a result, these simulations are not as susceptible to the chaotic variability inherent in genesis that complicates comparisons between current and future climates in other long-term simulations (Done et al. 2014), and they are not influenced by the initial conditions as shorter simulations might be.

2. Methods

a. Overview

This work uses a continental domain convection-permitting regional climate model (Liu et al. 2017) to assess the thermodynamic effects of climate change on hurricane intensity in the Gulf of Mexico and the U.S. East Coast. This is accomplished by running the Weather Research and Forecasting (WRF) Model forced with boundary conditions from ERA-Interim for the 13-yr period 2001–13, and again for a future climate after perturbing the same boundary conditions with the climate change signal derived from the multimodel mean change signal from the most recent Coupled Model Intercomparison Project [phase 5 of CMIP (CMIP5)]. The output from these simulations is then used as input to a hurricane-tracking algorithm. This combination is able to successfully simulate and track hurricanes from the current climate, and these tracks are compared with the observed NHC "best track" hurricane database (HURDAT) for the same period. While databases such as HURDAT are not free from errors themselves (Torn and Snyder 2012), they provide one of our best estimates in the current climate and therefore provide a useful check for the WRF simulations. The use of observed SSTs and the fact that the simulated tracks closely follow the real tracks mean that the SSTs the WRF atmosphere interacts with may have a reasonable cold wake embedded in them; however, this wake will not change dynamically in the future. The changes in these same tracks are then assessed for statistically significant changes in the mean of the maximum wind speeds, the radius of 33 $m\,s^{-1}$ winds, the translation speed of the cyclone, a cyclone damage potential index that combines these three metrics, the central pressure deficit, and finally the mean of the maximum precipitation amounts associated with hurricanes.

b. Regional climate model

We use the Weather Research and Forecasting Model, version 3.4.1, to simulate 13 years of current and future climate. These simulations are described and examined in greater detail in Liu et al. (2017), and an overview is provided here. Data from the WRF simulations are available online (Rasmussen and Liu 2017). The simulation domain covers the contiguous United States (CONUS) and portions of Canada and Mexico (Fig. 1) with a 4-km grid. This domain is 5440 km (east–west) by 4064 km (north–south). The model was set up with 51 vertical levels and the model top was set at 50 hPa. The parameterizations used were the Thompson aerosol-aware microphysics (Thompson and Eidhammer 2014), the Yonsei University (YSU) planetary boundary layer (Hong et al. 2006), the Rapid Radiative Transfer Model for GCMs (RRTMG) (Iacono et al. 2008), and the Noah land surface model with multiparameterization options (Noah-MP; Niu et al. 2011). A surface-layer option sometimes used to decrease surface friction over oceans during high winds (isftcflx) was left off because the initial focus of these simulations was not for hurricanes. Similarly, the WRF NWP diagnostics flag was not turned on, so the "maximum" wind speeds reported in this study are the maximum over a region of interest from the model instantaneous wind speeds. Because of these settings, we evaluate both the 10-m wind speeds and the 850-hPa wind speeds here. Spectral nudging was applied to the lowest wavenumbers above the boundary layer, and has been shown to retain regional climate extremes while remaining faithful to historical environmental conditions (Otte et al. 2012). The spectral nudging coefficient used was more than 6 times smaller than the default spectral nudging coefficient used in WRF to minimize the impact, and only scales on the order of 2000 km and greater were nudged.

The current climate simulations were performed for the period October 2000 through September 2013 with initial and boundary conditions from the ERA-Interim dataset (Dee et al. 2011). The ERA-Interim data have a 6-hourly time interval and a 0.7° spatial grid. Sea surface temperatures (SSTs) were also taken from the ERA-Interim dataset for the lower boundary condition throughout the simulation.

The future simulations were forced with the same input data after adding a climate change signal to the data using the pseudo–global warming (PGW) method (Schär et al. 1996; Rasmussen et al. 2011). In these simulations we applied a PGW change for the following input variables: zonal and meridional wind speed, sea level pressure, geopotential height, air temperature, relative humidity, and sea surface temperature as well as initial soil temperatures and the bottom boundary condition in the soil. We also modified the inputs to the radiative transfer scheme to account for changes in greenhouse gases. We compute the change signal over a 95-yr time period using data from the representative

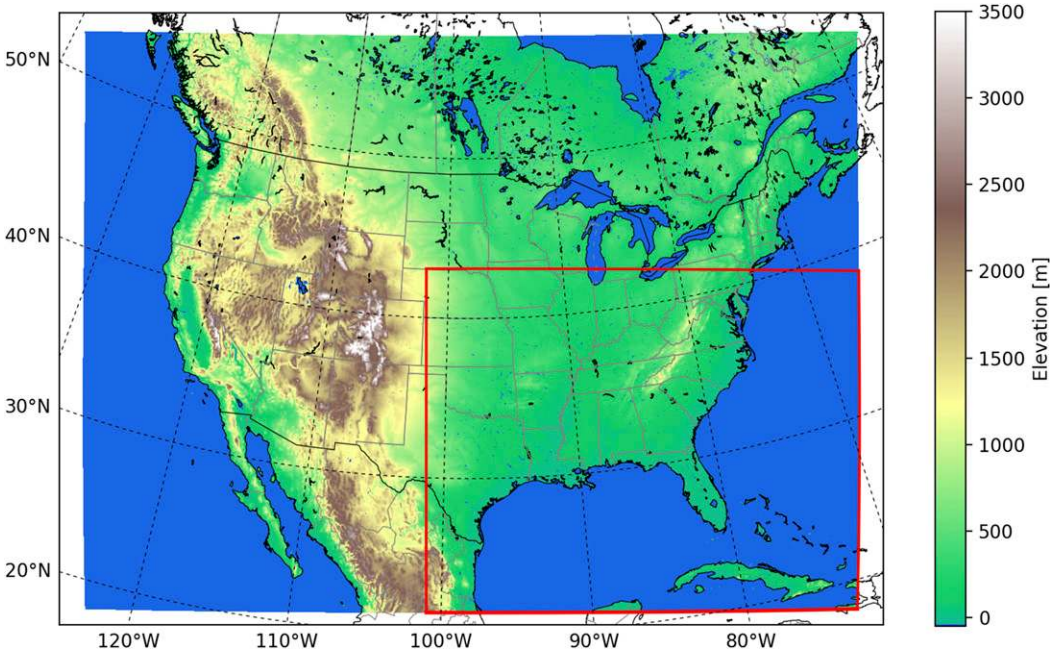

FIG. 1. Map of topography across the full WRF domain (color-shaded region). The region of focus in this study is outlined by the red box.

concentration pathway 8.5 (RCP8.5) scenario for 19 models in the CMIP5 archive. This is calculated by averaging the period 2070–99 and subtracting from it the average over the period 1976–2005. This change signal is calculated independently for every variable at every grid point in space, and for every month of the year. Changes are temporally interpolated between month midpoints. For example, the change signal for 15 May of all years is computing by averaging the change signal over the period 1–30 May. The resulting change signal has a mean warming signal of 3°–6°C and an increase in water vapor mixing ratio of 20%–40%, consistent with the Clausius–Clapeyron relationship. For more details see Liu et al. (2017).

Aside from temperature and humidity changes, the PGW changes in the boundary conditions are relatively modest. The changes in SSTs are nearly constant in space and time with an increase of 3.2 K over the analysis domain from June through October. Wind shear has a slight increase over the southern portion of the domain that is stronger in June through September and weaker in October. Mean meridional wind is almost unchanged. Mean zonal wind at sea level is nearly unchanged ($<1\,\mathrm{m\,s^{-1}}$), and zonal winds at 200 hPa increase by $1–5\,\mathrm{m\,s^{-1}}$.

The increases in atmospheric temperature and water vapor mixing ratio are shown in Fig. 2. Up to 200 hPa, the temperature changes range from 4 to 6 K, with the greatest increases occurring between 400 and 200 hPa. The enhanced warming at higher elevations increases the atmospheric stability and is a consistent characteristic across climate model projections as a result of increased convective activity in the tropics, which enhances upper-level heating through latent heat releases (Hill and Lackmann 2011). This is clearly an important stability influence in future simulations and is important to include. Similarly, Kang and Elsner (2015) illustrated the trade-offs between the frequency and intensity of hurricanes resulting from the change in stability. The change in temperature through the column does not vary much over time, although the increase in stability is slightly greater in September and October than it is in July and August. Also shown in Fig. 2 is the change in water vapor mixing ratio. Mixing ratio increases throughout the column, with the greatest increases near the surface ($4\,\mathrm{g\,kg^{-1}}$). Mixing ratio increases are greater in July, August, and September, with slightly larger increases in September. The increase in moisture provides a greater source of potential energy in the form of increased condensational heating.

c. *Tracking algorithm*

The tracking algorithm is based on surface pressure and 10-m height wind speeds as diagnosed by WRF. These fields are available on an hourly time step for the duration of the simulation. The resulting tracks were examined manually to confirm that they coincided with hurricanes in the HURDAT database and that

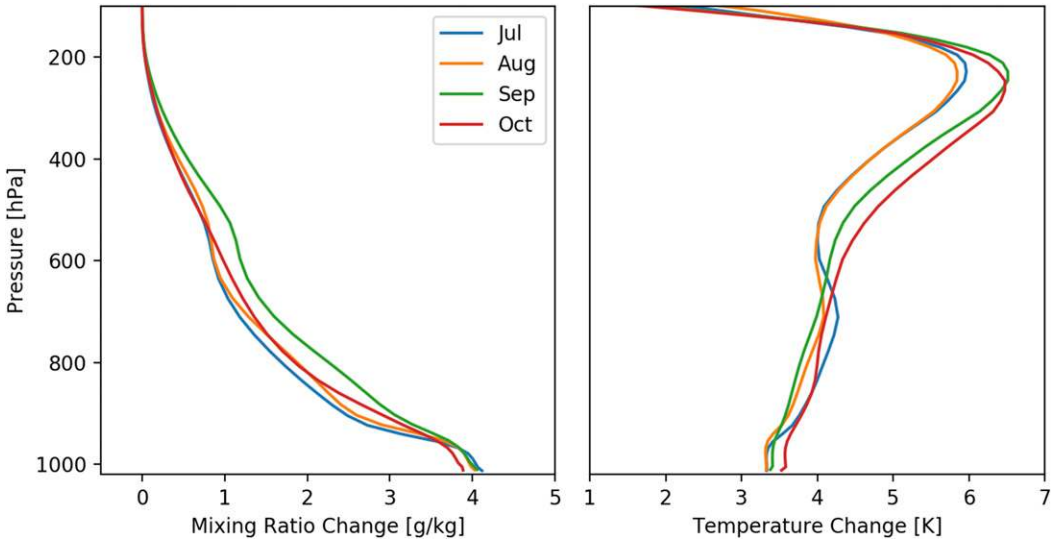

FIG. 2. Vertical profiles of changes in (left) water vapor mixing ratio and (right) temperature over the Gulf of Mexico in the WRF simulations for July, August, September, and October.

hurricanes in the HURDAT database were not missed by the tracking algorithm. In this manual step, tracks in the WRF simulations that were not present in the HURDAT database typically formed over land, at higher latitudes, or too early in the season to be considered tropical cyclones as part of this study, and they were removed from further analysis.

Objective tracking was performed using thresholds for wind speed and surface pressure. We initiate tracking of a point when the surface pressure falls 27 hPa below the 13-yr maximum pressure at a given point and the maximum 10-m wind speed in the surrounding 400 km × 400 km box exceeds 25 m s^{-1}. Points continue to be tracked from one time step to the next by searching a 400-km box around the previous point for the minimum pressure anomaly. As long as this minimum surface pressure remains 17 hPa below the long-term maximum and the maximum wind speed remains above 15 m s^{-1}, the point is recorded and tracking continues. Two points in sequential time steps are considered to be part of the same track if they fall within 400 km of each other. Manual analysis confirmed that vorticity and temperature were not required to adequately track the storms in these simulations, although using temperature may have allowed some nontropical tracks to be excluded automatically.

For each point along the track, storm statistics are calculated using data from the 400 km × 400 km region surrounding the point of minimum pressure. The maximum wind speed and precipitation rates are simply the maximum values in the 400 km × 400 km region. The minimum pressure is the minimum pressure in the region, by definition at the center of the region. The translation speed is calculated from the distance between the current track center and the previous track center divided by the tracking time interval (3600 s). The radius of 33 m s^{-1} winds is computed by first finding the easternmost and westernmost grid cells that exceed 33 m s^{-1} winds in every row of model grid cells in the region. The distance between each of these points and the track center is then computed, and the radius is determined as the average distance to all of these points. Finally, the cyclone damage potential (CDP) is computed following Holland et al. (2016). This relationship has been developed based on historical storm damage costs to relate maximum winds v_m, radius of hurricane-force winds R_h, and the storm translation speed v_t to damage potential as follows:

$$\mathrm{CDP} = 7.4\,\frac{\left[\left(\frac{v_m}{33}\right)^3 + \left(\frac{R_h}{18.5}\right)\right]}{v_t}.$$

3. Results

The WRF simulations were able to produce similar hurricane tracks for 30 of the 32 hurricanes in the HURDAT database whose track centers reached 400 km from the edges of the domain. We do not evaluate other tracks because the model does not have enough space to adequately simulate the storm without interference from the relatively coarse boundary conditions. Of these 30 tracks, one was only present in the PGW simulation (Gaston in 2004) and one was only

present in the current climate simulation (Claudette in 2003). The two tracks missing entirely were Hurricane Charley (2004) and Hurricane Erika (2003). From the remaining 28 tracks, three had relatively large changes in the track location between the current climate and the PGW simulation, two were not close enough to the HURDAT track, and one was too close to the eastern boundary. The remaining 22 tracks are analyzed in this paper.

The 22 best-simulated tracks are shown in the current climate alongside the HURDAT track in Fig. 3. The maps illustrate that WRF was able to simulate these track locations accurately in the current climate. The biggest differences between the WRF and HURDAT tracks are seen at either end of the tracks. Frequently the WRF tracks do not start until further into the domain than the HURDAT tracks, or they stop before the HURDAT track stops. These could be partly due to the thresholds applied in the tracking algorithm, as the HURDAT tracks include periods when the storm is only a tropical storm or depression, while the WRF tracks were limited to stronger tropical cyclones. In addition, the boundary conditions do not include hurricane force winds because of the coarse nature of the reanalysis; as a result, the WRF simulation needs some time for its internally generated circulation to develop hurricane-force winds. The simulated track locations are also partially controlled by the spectral nudging applied to the upper atmosphere. However, this does not entirely constrain simulated track locations as evident by the tracks that do diverge from the observed tracks.

In addition to the strong match of track locations, WRF is able to reliably simulate the radius of hurricane-force winds, although it produces slightly lower intensities (higher central pressures) and WRF does not simulate the most intense winds seen in the HURDAT database (Fig. 4). The statistical distributions of radii, pressures, and maximum wind speeds in both the HURDAT and WRF tracks are shown in Fig. 4. While the wind speed distributions in WRF and HURDAT overlap considerably, the WRF current climate simulations have fewer points with wind speeds greater than $45\,m\,s^{-1}$, and do not produce any wind speeds greater than $55\,m\,s^{-1}$. Regional climate models are typically not able to simulate the highest wind speeds because the grid spacing does not permit them to resolve the most extreme motions. While this problem is substantially reduced by convection-permitting grid spacing, it has been shown that even simulations on a 2-km grid do not quite match the intensity of observations for the most extreme convective events (Lind et al. 2016), with coarser resolutions being weaker. Similarly, Davis et al. (2008) showed that, for example, rapid intensification is not well simulated until model grid spacing decreases to 1 km.

The current and PGW track locations are very similar (Fig. 5). It is important that the current and future track locations are similar so that changes can be clearly attributed to thermodynamic effects rather than being due to semirandom variability if the tropical cyclone interacts with different surfaces in the future simulation. As mentioned above, the three tracks in which the future WRF simulation differed from the current simulation were removed from analysis because we did not want variations in track location to affect the results. For example, if future tracks happened to be substantially closer or farther from land the change in drag and latent heating might change the cyclone intensity independent of the thermodynamically driven changes.

Statistics for all tracks' wind speed, radius, translation speed, cyclone damage potential, central pressure, and rainfall rate are presented in Table 1. The values in the table are averaged along the track for each hurricane and averaged across all track points for the total. The maximum wind speeds increased in 15 of the 22 tracks, and statistical significance is based on the Student's t test for independent samples. Because these samples (current and PGW track points) are not truly independent, the paired Student's t test could be used and would likely find more changes to be statistically significant as the current test conflates within storm variability with sampling variability. However, there is no direct one-to-one connection between track points because of chaotic variability in the two simulations. Because of this we opted for the more conservative Student's t test. Using this test, increases in maximum wind speed are statistically significant ($p < 0.05$) in nine tracks (Table 1 and Fig. 6). A decrease in maximum wind speed is only statistically significant in one track, and the combined points from all tracks show a statistically significant increase ($p < 0.01$) from 32 to $34\,m\,s^{-1}$.

In contrast, the mean radius does not significantly change when averaged across all track points (Table 1). Individual storms have statistically significant increases (four storms) and decreases (two storms) in radii. This could mean that certain types and locations of storms will increase or decrease their radii; however, the present data are not sufficient to test this hypothesis, and initial exploratory analysis did not indicate any such relationship.

The translation speed of the tracks has a statistically significant decrease ($p < 0.01$) across all tracks from 7 to $6.4\,m\,s^{-1}$ (Table 1). Of the 22 individual tracks, 14 have decreases in translation speed, although only 3 of those are statistically significant.

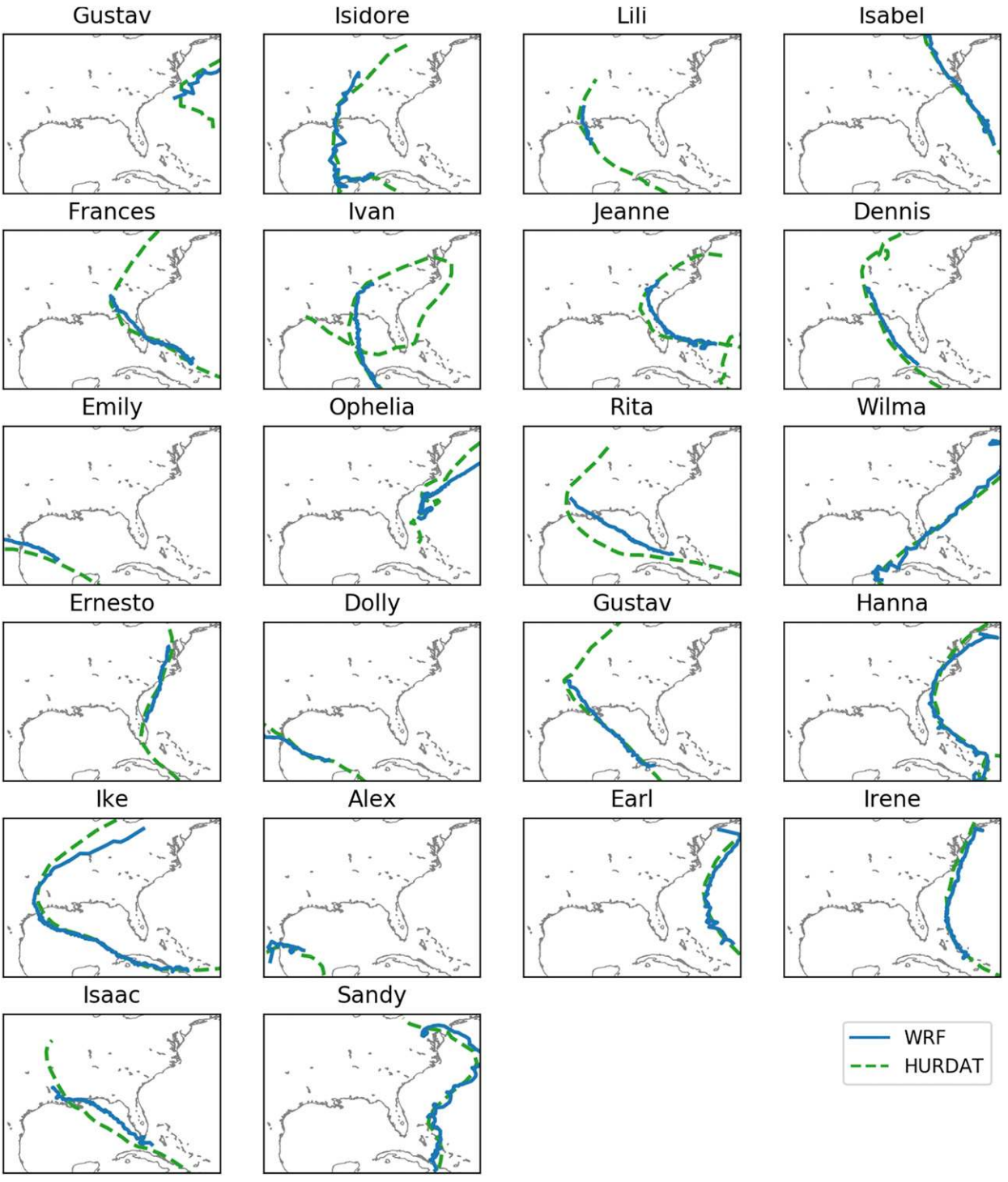

FIG. 3. Maps of all 22 tracks for which the WRF simulations (solid blue) matched the HURDAT tracks (dashed green) and the PGW WRF tracks were similar to the current climate tracks. Coastlines and lakes are shown in gray for reference.

The combined effect of the three variables is represented in the CDP index, which has a statistically significant increase ($p < 0.01$) from 5.3 to 5.9 (Table 1). CDP increased in 17 of the individual tracks, and this increase is statistically significant in 6 of those tracks ($p < 0.01$). CDP decreased in 5 tracks, even though none of these are statistically significant.

The intensity of hurricanes is often measured by the magnitude of the central pressure deficit and in these

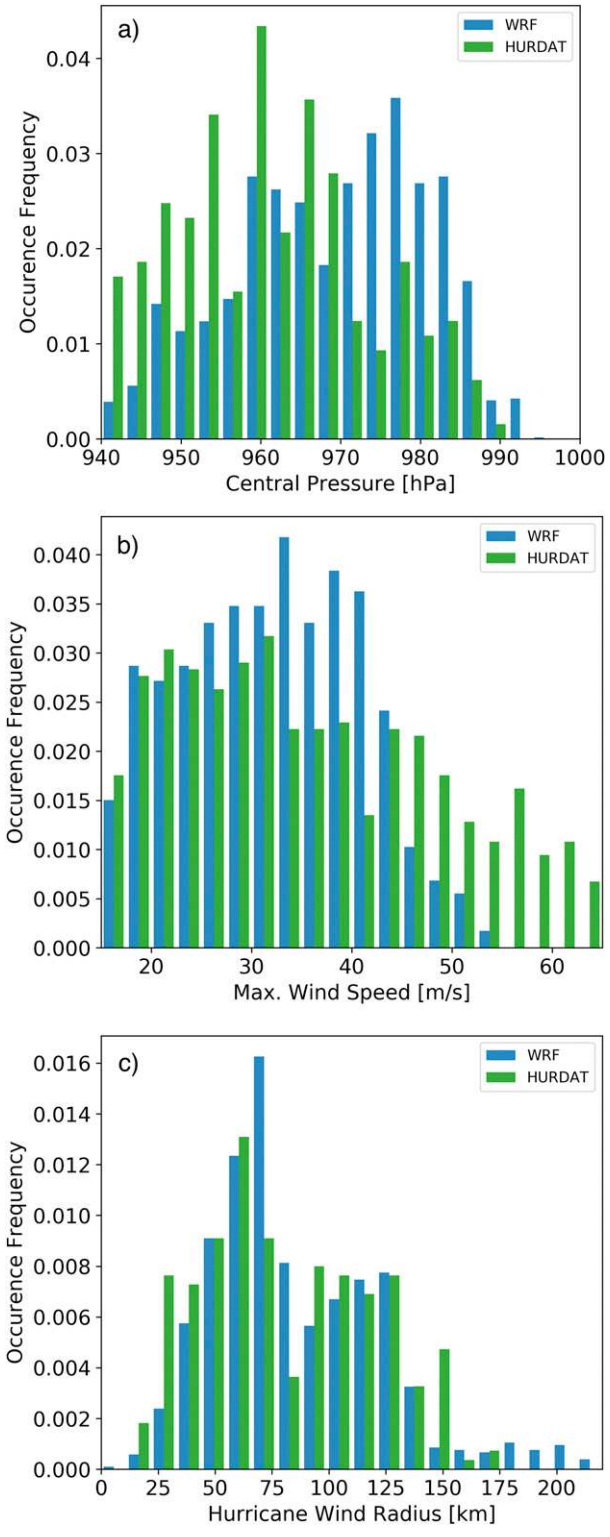

FIG. 4. Histogram of (a) central pressure, (b) maximum wind speed, and (c) radius of hurricane-force wind ($33\,m\,s^{-1}$) within the domain in the HURDAT database (green) and the WRF current climate simulation (blue).

simulations, averaged across all tracks, the central pressure decreased from 966 to 962 hPa ($p < 0.01$). Decreases are present in 16 of the tracks, with statistical significance ($p < 0.05$) in 12 of those tracks. Statistically significant increases ($p < 0.05$) are only present in 2 tracks.

The average maximum rainfall rate increased by 24% when averaged across all tracks from 83 to $103\,mm\,h^{-1}$ ($p < 0.01$). The average maximum rainfall rate increased in all tracks, and this difference is statistically significant for all but one track ($p < 0.05$), with all but two of those being significant with $p < 0.01$.

Combining all track points together means that longer lived storms will have a greater influence on the results, but such storms will also have a greater impact on society, so this seems like a reasonable implicit weighting factor. Changes in track length between the two simulations are not significant for most storms (Fig. 5), so such changes are not likely to influence the final result. To investigate this further, we subset the current and future tracks to only those points that corresponded to the same points in time. This change does not significantly change the mean values or the change signal much, but it does result in an increase from 9 to 13 tracks for which the increase in maximum wind speed is statistically significant. This also increases the number of tracks with statistically significant decreases in minimum pressure from 12 to 14, the two tracks with significant increases in minimum pressure are unchanged.

For wind speed, CDP, and precipitation, arguably the most important changes for societal impacts are those that occur at the highest end of the scale. We illustrate the changes in the statistical distribution of these values through histograms in Figs. 6, 7, and 8. The most significant increases exist at the highest wind speeds, with decreases in relative occurrence frequency between 25 and $45\,m\,s^{-1}$ and substantial increases in frequency for wind speeds between 45 and $65\,m\,s^{-1}$ (Fig. 6). To specifically isolate cyclones that would be considered category 3 and above hurricanes, we compare the occurrence frequency of winds above and below $50\,m\,s^{-1}$. There is a substantial increase in the frequency of occurrence of winds greater than $50\,m\,s^{-1}$ from 2% of all points in the current climate to 9% of points in future climate. Similarly, high CDP values increase in frequency for most bins with a CDP greater than five, and decrease in relative frequency for most bins less than five (Fig. 7). As with wind speeds, the greatest changes are in the most extreme (CDP > 9) bin, which increases in relative frequency from 7% to 17%. Finally, precipitation also shows a large increase in the frequency of the most intense precipitation events (Fig. 8). There is a large increase in the relative occurrence frequency for precipitation rates greater than $100\,mm\,h^{-1}$.

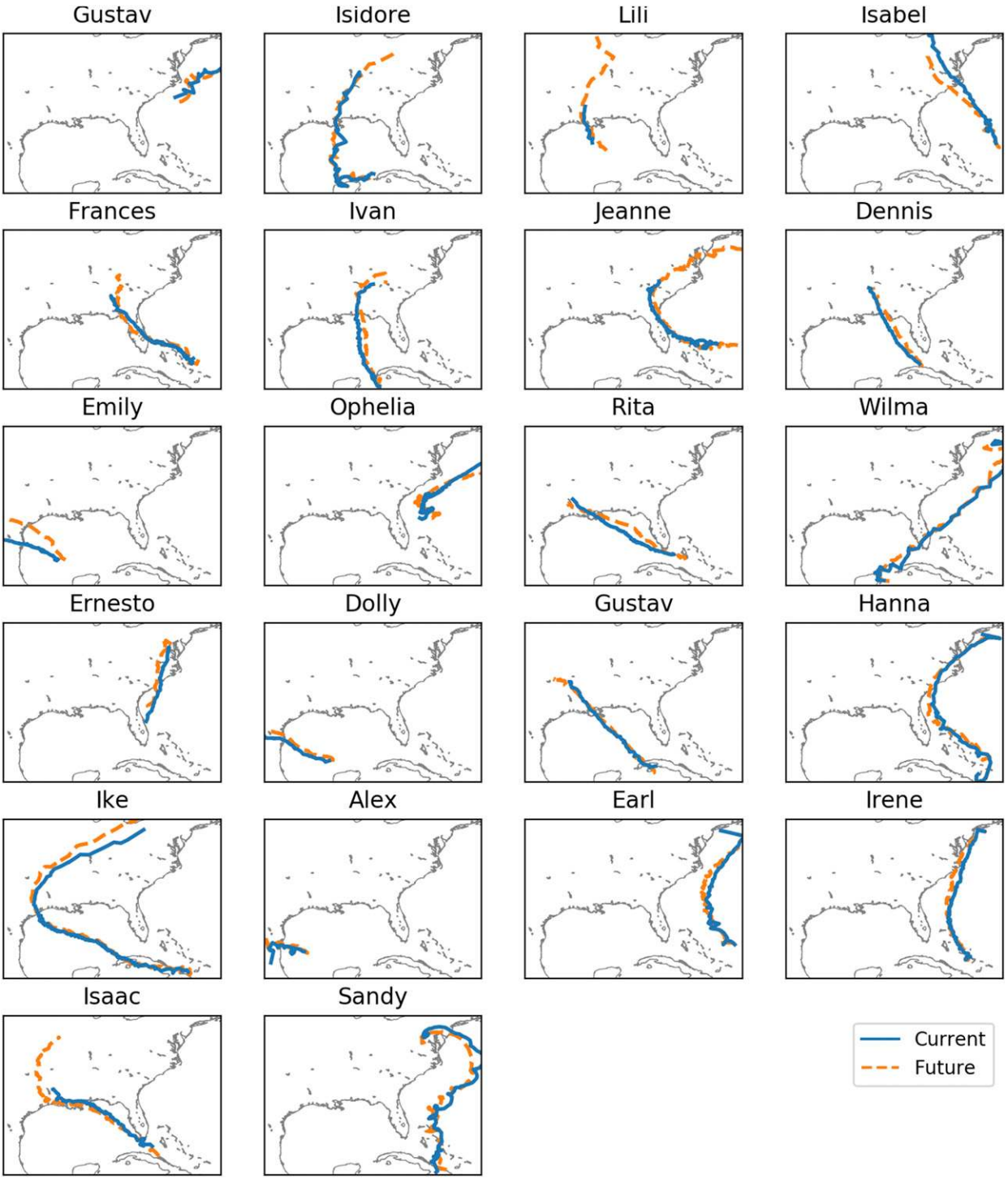

FIG. 5. Tracks for all 22 storms from the current climate (solid blue) and PGW future climate (dashed orange).

4. Discussion

a. Physical changes

The results presented in this study are consistent with prior studies, which suggest that the mean hurricane intensity may not increase much, but the hurricanes with the highest wind speeds may become a larger fraction of the number of storms. The typical minimum sea level pressure and maximum wind speeds show only modest changes in our study, while more extreme winds are

TABLE 1. Statistics for all storms and the combined values across all tracks. Wind speed is the average of the hourly maximum wind speeds, and rainfall is the average of the hourly maximum rainfall in the region around each point. Statistically significant differences are noted by one and two asterisks for $p < 0.05$ and $p < 0.01$, respectively.

Name	Period	Wind speed ($m\,s^{-1}$)	Radius of 33 $m\,s^{-1}$ wind (km)	Translation speed ($m\,s^{-1}$)	CDP	Central pressure (hPa)	Rainfall rate ($mm\,h^{-1}$)
Gustav (2002)	Current	25	71	7.8	4.3	975	90
	Future	29*	73	8.3	4.8	969*	123**
Isidore (2002)	Current	23	84	5.2	4.5	979	95
	Future	25**	94	6.4	5.8	975**	101
Lili (2002)	Current	25	46	8.1	0.6	977	62
	Future	25	48	9	2.1	975	69*
Isabel (2003)	Current	32	114	7.5	6.3	963	81
	Future	34	124*	6.8	7.4**	958*	97**
Frances (2004)	Current	34	82	5.9	5.1	966	81
	Future	33	81	5.7	5.3	965	95**
Ivan (2004)	Current	35	106	6.8	6.4	963	91
	Future	36	100	6.4	6.3	962	121**
Jeanne (2004)	Current	29	67	8.8	3.9	971	76
	Future	30	71	7.1*	5.1**	967*	92**
Dennis (2005)	Current	32	56	7.1	3.7	966	83
	Future	32	53	7.7	3.4	971*	116**
Emily (2005)	Current	34	62	6.1	4.3	969	74
	Future	36	45**	6	3.8	967	111**
Ophelia (2005)	Current	38	58	5.9	4.2	968	64
	Future	42**	57	3.3**	5.5**	956**	88**
Rita (2005)	Current	36	61	5.6	4.6	964	98
	Future	35	60	5.7	4.9	967	124**
Wilma (2005)	Current	26	121	7.2	6.5	976	94
	Future	30**	116	6.3	6.5	967**	112**
Ernesto (2006)	Current	27	52	6.9	3.2	980	84
	Future	25*	75	6.2	4.2	983*	105**
Dolly (2008)	Current	31	35	4.7	3	964	90
	Future	35*	44**	4.5	3.9**	955**	100*
Gustav (2008)	Current	30	84	6.9	5.1	960	83
	Future	28	77	6.3	5	962	104**
Hanna (2008)	Current	26	72	8.4	3.5	974	80
	Future	27	49**	8.4	3.4	973	106**
Ike (2008)	Current	37	111	8.1	7.2	953	92
	Future	42**	112	6.7**	7.7	941**	123**
Alex (2010)	Current	27	117	7.4	5.9	977	101
	Future	27	102	7.2	5.9	976	129**
Earl (2010)	Current	34	93	10.1	5.2	963	86
	Future	42**	108**	10.6	6.9**	953**	104**
Irene (2011)	Current	40	106	7.9	6.4	948	73
	Future	43**	117*	7.4	7.4**	937**	88**
Isaac (2012)	Current	28	51	5.5	3.7	974	78
	Future	32**	52	5.7	4.5	965**	100**
Sandy (2012)	Current	32	146	7.8	7.3	956	73
	Future	33	147	7.6	7.5	952*	94**
All data	Current	32	86	7	5.3	966	83
	Future	34**	87	6.4**	5.9**	962**	103**

much more common, and the associated cyclone damage potential index increases noticeably. The increase in precipitation is the most consistent change across all storms, with the largest increases present for the most extreme precipitation rates.

The decrease in storm translation speed is small, but statistically significant, and is likely caused by the large-scale changes in circulation imposed with the PGW forcing. Tropical cyclone tracks are primarily driven by the environmental flow, known as the steering flow. Only in regions of weak environmental flow can other factors become important such as the effects of asymmetric convection in the cyclone, and the influence of SST gradients or coastlines. To explain the future reduction

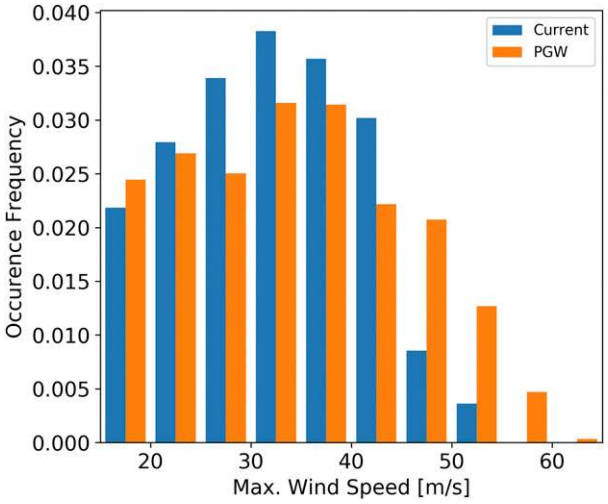

FIG. 6. Histogram of maximum wind speed for all points on all tracks from the current climate (blue) and PGW climate (orange) simulations.

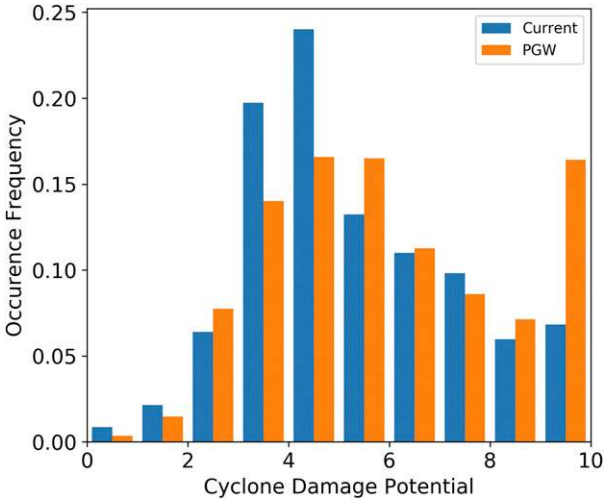

FIG. 7. As in Fig. 6, but for CDP.

in mean translation speed we therefore look to the future change in steering flow. The PGW change signal adds a mean circulation change, although small in magnitude. Liu et al. (2017) showed that the CMIP5 mean climate change added here contains a summer high pressure anomaly centered over the U.S. Northeast [see Figs. 2 and 3 in Liu et al. (2017)]. This drives an anomalous northeasterly flow of up to 1.5 m s^{-1} over the Atlantic and, to a lesser extent, the Gulf of Mexico. This introduces a slight relative headwind to the mean cyclone tracks and is likely the cause of the slight reduction in translation speed.

The change in precipitation is more pronounced, and is likely caused by a combination of the direct increase in atmospheric moisture and an increase in vertical motion. The PGW change signal adds up to 4 g kg^{-1} to the water vapor mixing ratio (Fig. 2), consistent with the Clausius–Clapeyron equation and the 3.5-K increase in air temperature. Averaging the water vapor mixing ratio in a moving window around each storm track shows a slightly larger increase in total column precipitable water (28%). This is greater than the increase in maximum precipitation rates (24%). In addition, there is a 7% increase in the maximum vertical updraft speeds, presumably due to local dynamical feedbacks caused by the increase in condensational heating from the additional moisture. While the change in maximum vertical motion and average precipitable water are not additive, the relative magnitude of these changes suggests that more of the increase in modeled precipitation rates is due to directly to the increase in atmospheric moisture, with a smaller component resulting from dynamical feedbacks.

b. *Methodological discussion*

Because this study used the PGW approach to assess the thermodynamic effects of climate change, it is difficult to make any inferences about the possible changes in the frequency of hurricanes in the future. The current and PGW simulations here both failed to simulate three observed storms strongly enough to be tracked. Their absence is likely not related to genesis, but rather to minor perturbations causing a simulation to not reach the threshold necessary to be tracked. In one case, Hurricane Erika did form inside the WRF domain but was only a tropical storm within the region according to HURDAT; as a result the WRF simulation may not be expected to create a strong enough storm to track with the 25 m s^{-1} maximum wind threshold used here. Hurricane Gaston also formed within the domain, but failed to do so in the current climate simulation. Similar to Erika, Gaston was only a category-1 hurricane, and only for a single data point in the HURDAT database. As such, random variability could again be enough to prevent it growing strong enough to track in the current climate simulation. There was one major hurricane absent from the simulations (Charley), which will be discussed further below. Because of the potential subjectivity surrounding which storms to include, we repeated the summary statistical calculations in Table 1 including points from the 28 storms that occurred in both WRF simulations. When including all storms the absolute value of the numbers changed slightly, but the relative magnitude of the changes and the statistical significance stayed the same.

This study has shown the utility of permitting the hurricanes to enter through the boundaries of the domain. It is important to note that only two HURDAT

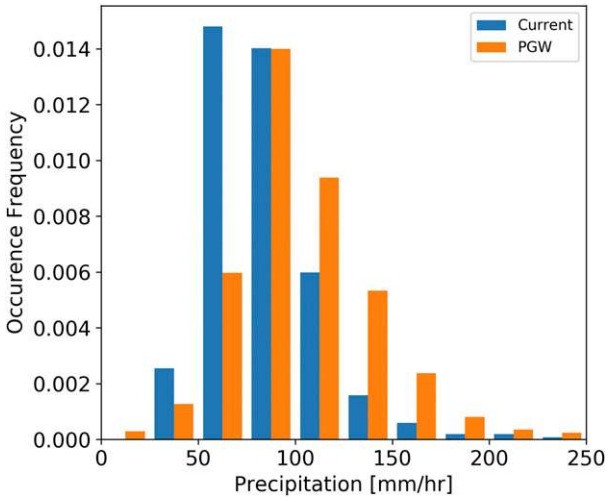

FIG. 8. As in Fig. 6, but for maximum precipitation rate in the region surrounding each track point.

tracks that crossed the WRF domain boundary were not simulated in one or both of our tests. Hurricane Claudette was simulated in the current climate, but not the PGW case. Claudette remained a tropical storm in the HURDAT database within this region, and it may have been simulated in the PGW case; it simply did not grow strong enough to track. In contrast, Hurricane Charley was a category-4 hurricane that was hurricane force when it crossed over the WRF domain boundary; however, it was not simulated in either the current or the PGW climate simulations. Charley was the second-costliest hurricane on record at the time, and it remains the eighth costliest (Blake et al. 2011) at the time this manuscript was written. Because of this, understanding why this was not simulated is important to understand the limitations of the method.

The problems in simulating Charley appear to come from the combination of hurricane features and the ERA-Interim forcing data themselves. Charley was a relatively fast-moving hurricane (translation speed of $8\,m\,s^{-1}$) with a narrow radius of hurricane-force winds (35 km) when it crossed the WRF Model boundary according to the HURDAT database. This means that the model boundary will not have a long period of time or a large area strongly influenced by Charley. This is compounded by a weak storm representation in the ERA-Interim dataset, due in part to the grid spacing of the dataset (0.7°). Notably, the grid spacing in ERA-Interim is larger than the radius of hurricane-force winds. Manual analysis confirmed that, in the ERA-Interim dataset, Charley is particularly weak when it crosses the WRF boundary. Wind speeds in ERA-Interim do not exceed $10\,m\,s^{-1}$, and the central pressure is greater than 1010 hPa until after Charley crosses the boundary. As a result, the boundary conditions do not strongly force the presence of a hurricane, and no such storm appears in the WRF simulation. This is a limitation of the methodology used with these boundary conditions, but it is not a problem that would affect the climate change signal of other storms because we do not try to evaluate changes in formation characteristics; as such, we do not consider this to weaken the results of this study.

One of the more important results of this paper is the large difference seen between different storms. Many past convection-permitting studies have focused on a single storm; however, in this study we show that individual storms may exhibit a decrease in wind speeds and intensity [e.g., Hurricane Ernesto (2006); Table 1], even if the average over all storms is a statistically significant increase. This may be mitigated somewhat by past studies frequently using multiple ensemble members to quantify some of that uncertainty, but it is possible that specific storms may have characteristics that lead to an increase or decrease in intensity in the future, regardless of how many simulations are performed. This would be particularly true if the large-scale change tends to push the future track into a region that is less conducive to strong storms (e.g., closer to land or cooler SSTs). This could explain the decreases in wind speeds found for Hurricane Katrina by Lynn et al. (2009). In our study, we excluded Katrina because it was one of two hurricanes that were not deemed to be well simulated; the wind speeds in Katrina did decrease in our simulations, although these decreases were not statistically significant. In another study, Lackmann (2015) reported decreases in the central pressure for Hurricane Sandy, with no reported change in winds. In the present study, we also found decreases in central pressure for Sandy, but only a small increase in wind speeds that was not statistically significant. While a detailed analysis of the change in each individual hurricane and its causes is beyond the scope of this study, initial comparisons found no clear indication that the interstorm differences are related to the local change in the SSTs or to hurricane characteristics in the current climate (e.g., radius or wind speed).

The ocean surface roughness setting used appears unlikely to be the reason we find only small changes in maximum wind speeds. To investigate this, we evaluate the 850-hPa maximum wind speeds using the same analysis presented for 10-m height winds, and we compare changes for different wind speeds. The changes in 850-hPa wind speeds are correlated with the change in 10-m height winds ($r = 0.84$), and the tracks that have statistically significant changes are almost identical. Using the 850-hPa wind speeds results in one additional track having a statistically significant increase in maximum

wind speeds and one additional track having a statistically significant decrease. In addition, the lack of a surface roughness limiter should have the most effect on the fastest wind speeds; however, the fastest wind speeds exhibit the greatest increase in frequency in our study.

5. Conclusions

Long-term convection-permitting simulations of hurricanes offer an important methodological approach for climate change studies. High resolution makes it possible to turn off the convective parameterizations in these models and to simulate the relevant dynamics explicitly, removing a large source of uncertainty in many model simulations. Although the computational cost of such models currently imposes limits on their use, future advances in computing capacity will likely enable large ensembles, longer-duration simulations, and larger domains appropriate for the study of genesis.

We have presented hurricane tracks from two 13-yr WRF simulations performed on a 4-km, convection-permitting grid. This convection-permitting simulation, driven by reanalysis data, is able to realistically represent most of the major hurricanes in the current climate when requiring the hurricanes to be initialized in the domain through the boundary conditions. Past studies have typically been limited to studying one or a few hurricanes because of computational costs, and thus they have positioned the domain optimally to simulate each individual event and have initialized the model with the storm already formed. Here we show the utility of a single large domain (initially created for water cycle studies over the CONUS; Liu et al. 2017) for hurricane studies. In the current study, the hurricanes are imposed by the boundary conditions. Several hurricanes do form spontaneously inside the domain with no direct interaction with the boundaries, but these often do not match the HURDAT tracks well. Of note, this study also found significant differences in the changes simulated for different hurricanes, indicating the importance of evaluating multiple hurricanes when trying to draw more general conclusions.

The thermodynamic effects of climate change on a 13-yr record of hurricanes were simulated using a pseudo–global warming methodology. This approach showed a statistically significant increase in the mean of the maximum wind speeds, a damage potential index, and associated maximum precipitation and a statistically significant decrease in the storm translation speeds and the minimum central pressures. Importantly, these simulations had a large increase in the frequency of occurrence of wind speeds over $50\,\mathrm{m\,s^{-1}}$. This suggests that the frequency of category 3, 4, and 5 hurricanes may increase relative to the frequency of category 1 and 2 hurricanes, although this study does not predict changes in genesis, and it is possible that either weaker storms will develop into category 1 and 2 hurricanes or that more weak tropical cyclones will form in the future, thus keeping the relative frequencies unchanged. These results are generally consistent with Knutson et al. 2013, who added a similar climate perturbation based on the CMIP5 ensemble to a regional climate model. It is important to note that the current study constrains both hurricane genesis and track locations through the boundary conditions and spectral nudging. It is possible that dynamic effects in a future climate could shift track locations into regions less conducive for hurricane intensification and thus negate the changes simulated here.

This study is consistent with the idealized findings of Hill and Lackmann (2011), which suggested increases in the most intense hurricanes with a different PGW experiment. The current study shows that these findings hold for simulations of historical hurricanes, not just idealized hurricanes. Because this study combined both changes in water vapor and changes in stability, it provides support for the suggestion that the increases in water vapor and thus latent heat feedbacks may dominate over the increases in stability as put forward by Hill and Lackmann (2011).

These simulations showed significant increases in maximum rainfall rates by approximately 24%. Rainfall rates are the only statistic that showed increases across all storms and statistical significance in the change signal for all but one storm. This increase is consistent with the increase in water vapor predicted by the Clausius–Clapeyron equation, indicating that future hurricanes are efficient in their conversion of increases in water vapor to precipitation. This indicates that the increase in maximum rainfall rates is a reliable change as predicted by the 19-CMIP5-model mean change in climate used in these simulations. This is important because flooding caused by heavy rainfall is frequently one of the dominant impacts [e.g., Hurricanes Allison (2001), Irene (2011), and Harvey (2017)].

Acknowledgments. We would like to acknowledge high-performance computing support from Yellowstone (http://n2t.net/ark:/85065/d7wd3xhc) provided by NCAR Computational and Information Systems Laboratory's NCAR Strategic Capability allocation. The creation of the 4-km current and future 13-yr CONUS simulations were supported by the National Science Foundation (Grant AGS-0753581) under the NCAR Water System Program. The National Center for Atmospheric Research is sponsored by the National Science Foundation.

ERA-Interim data provided courtesy of ECMWF (data are available online at http://apps.ecmwf.int/datasets/data/interim-full-daily/). Analysis of the simulations was supported by Det Norske Veritas Germanischer Lloyd (DNV GL).

REFERENCES

Blake, E. S., C. W. Landsea, and E. J. Gibney, 2011: The deadliest, costliest and most intense United States tropical cyclones from 1851 to 2010 (and other frequently requested hurricane facts). NOAA Tech. Memo. NWS NHC-6, 47 pp.

Davis, C., and Coauthors, 2008: Prediction of landfalling hurricanes with the Advanced Hurricane WRF Model. *Mon. Wea. Rev.*, **136**, 1990–2005, https://doi.org/10.1175/2007MWR2085.1.

Dee, D. P., and Coauthors, 2011: The ERA-Interim reanalysis: Configuration and performance of the data assimilation system. *Quart. J. Roy. Meteor. Soc.*, **137**, 553–597, https://doi.org/10.1002/qj.828.

Done, J. M., C. L. Bruyere, M. Ge, and A. Jaye, 2014: Internal variability of North Atlantic tropical cyclones. *J. Geophys. Res. Atmos.*, **119**, 6506–6519, https://doi.org/10.1002/2014JD021542.

Emanuel, K., 1987: The dependence of hurricane intensity on climate. *Nature*, **326**, 483–485, https://doi.org/10.1038/326483a0.

——, 2005: Increasing destructiveness of tropical cyclones over the past 30 years. *Nature*, **436**, 686–688, https://doi.org/10.1038/nature03906.

——, 2007: Environmental factors affecting tropical cyclone power dissipation. *J. Climate*, **20**, 5497–5509, https://doi.org/10.1175/2007JCLI1571.1.

——, 2011: Global warming effects on U.S. hurricane damage. *Wea. Climate Soc.*, **3**, 261–268, https://doi.org/10.1175/WCAS-D-11-00007.1.

Frank, W. M., and E. A. Ritchie, 2001: Effects of vertical wind shear on the intensity and structure of numerically simulated hurricanes. *Mon. Wea. Rev.*, **129**, 2249–2269, https://doi.org/10.1175/1520-0493(2001)129<2249:EOVWSO>2.0.CO;2.

Guha-Sapir, D., R. Below, and P. Hoyois, 2017: EM-DAT: The CRED/OFDA International Disaster Database. Université Catholique de Louvain, http://www.emdat.be/.

Hill, K. A., and G. M. Lackmann, 2011: The impact of future climate change on TC intensity and structure: A downscaling approach. *J. Climate*, **24**, 4644–4661, https://doi.org/10.1175/2011JCLI3761.1.

Holland, G. J., 1997: The maximum potential intensity of tropical cyclones. *J. Atmos. Sci.*, **54**, 2519–2541, https://doi.org/10.1175/1520-0469(1997)054<2519:TMPIOT>2.0.CO;2.

——, and C. L. Bruyère, 2014: Recent intense hurricane response to global climate change. *Climate Dyn.*, **42**, 617–627, https://doi.org/10.1007/s00382-013-1713-0.

——, J. M. Done, M. Ge, and R. Douglas, 2016: An index for cyclone damage potential. *32nd Conf. on Hurricanes and Tropical Meteorology*, San Juan, PR, Amer. Meteor. Soc., 5C.8, https://ams.confex.com/ams/32Hurr/webprogram/Paper293660.html.

Hong, S.-Y., Y. Noh, and J. Dudhia, 2006: A new vertical diffusion package with an explicit treatment of entrainment processes. *Mon. Wea. Rev.*, **134**, 2318–2341, https://doi.org/10.1175/MWR3199.1.

Hoyos, C. D., P. A. Agudelo, P. J. Webster, and J. A. Curry, 2006: Deconvolution of the factors contributing to the increase in global hurricane intensity. *Science*, **312**, 94–97, https://doi.org/10.1126/science.1123560.

Iacono, M. J., J. S. Delamere, E. J. Mlawer, M. W. Shephard, S. A. Clough, and W. D. Collins, 2008: Radiative forcing by long-lived greenhouse gases: Calculations with the AER radiative transfer models. *J. Geophys. Res.*, **113**, D13103, https://doi.org/10.1029/2008JD009944.

Kang, N.-Y., and J. B. Elsner, 2015: Trade-off between intensity and frequency of global tropical cyclones. *Nat. Climate Change*, **5**, 661–664, https://doi.org/10.1038/nclimate2646.

Knutson, T. R., and Coauthors, 2010: Tropical cyclones and climate change. *Nat. Geosci.*, **3**, 157–163, https://doi.org/10.1038/ngeo779.

——, and Coauthors, 2013: Dynamical downscaling projections of twenty-first-century Atlantic hurricane activity: CMIP3 and CMIP5 model-based scenarios. *J. Climate*, **26**, 6591–6617, https://doi.org/10.1175/JCLI-D-12-00539.1.

——, J. J. Sirutis, S. T. Garner, G. A. Vecchi, and I. M. Held, 2008: Simulated reduction in Atlantic hurricane frequency under twenty-first-century warming conditions. *Nat. Geosci.*, **1**, 359–364, https://doi.org/10.1038/ngeo202.

Kossin, J. P., K. A. Emanuel, and G. A. Vecchi, 2014: The poleward migration of the location of tropical cyclone maximum intensity. *Nature*, **509**, 349–352, https://doi.org/10.1038/nature13278.

Lackmann, G. M., 2015: Hurricane Sandy before 1900 and after 2100. *Bull. Amer. Meteor. Soc.*, **96**, 547–560, https://doi.org/10.1175/BAMS-D-14-00123.1.

Lind, P., D. Lindstedt, E. Kjellström, and C. Jones, 2016: Spatial and temporal characteristics of summer precipitation over central Europe in a suite of high-resolution climate models. *J. Climate*, **29**, 3501–3518, https://doi.org/10.1175/JCLI-D-15-0463.1.

Liu, C., and Coauthors, 2017: Continental-scale convection-permitting modeling of the current and future climate of North America. *Climate Dyn.*, **49**, 71–95, https://doi.org/10.1007/s00382-016-3327-9.

Lynn, B. H., R. Healy, and L. M. Druyan, 2009: Investigation of Hurricane Katrina characteristics for future, warmer climates. *Climate Res.*, **39**, 75–86, https://doi.org/10.3354/cr00801.

Mallard, M. S., G. M. Lackmann, A. Aiyyer, and K. Hill, 2013a: Atlantic hurricanes and climate change. Part I: Experimental design and isolation of thermodynamic effects. *J. Climate*, **26**, 4876–4893, https://doi.org/10.1175/JCLI-D-12-00182.1.

——, ——, and ——, 2013b: Atlantic hurricanes and climate change. Part II: Role of thermodynamic changes in decreased hurricane frequency. *J. Climate*, **26**, 8513–8528, https://doi.org/10.1175/JCLI-D-12-00183.1.

Mann, M. E., and K. A. Emanuel, 2006: Atlantic hurricane trends linked to climate change. *Eos, Trans. Amer. Geophys. Union*, **87**, 233–241, https://doi.org/10.1029/2006EO240001.

Mendelsohn, R., K. Emanuel, S. Chonabayashi, and L. Bakkensen, 2012: The impact of climate change on global tropical cyclone damage. *Nat. Climate Change*, **2**, 205–209, https://doi.org/10.1038/nclimate1357.

Neumann, J. E., and Coauthors, 2015: Climate change risks to US infrastructure: Impacts on roads, bridges, coastal development, and urban drainage. *Climatic Change*, **131**, 97–109, https://doi.org/10.1007/s10584-013-1037-4.

Niu, G.-Y., and Coauthors, 2011: The community Noah land surface model with multiparameterization options (Noah-MP): 1. Model description and evaluation with local-scale measurements. *J. Geophys. Res.*, **116**, D12109, https://doi.org/10.1029/2010JD015139.

Oouchi, K., J. Yoshimura, H. Yoshimura, R. Mizuta, S. Kusunoki, and A. Noda, 2006: Tropical cyclone climatology in a global-warming climate as simulated in a 20 km-mesh global atmospheric model: Frequency and wind intensity analyses. *J. Meteor. Soc. Japan*, **84**, 259–276, https://doi.org/10.2151/jmsj.84.259.

Otte, T. L., C. G. Nolte, M. J. Otte, and J. H. Bowden, 2012: Does nudging squelch the extremes in regional climate modeling? *J. Climate*, **25**, 7046–7066, https://doi.org/10.1175/JCLI-D-12-00048.1.

Rasmussen, R., and C. Liu, 2017: High resolution WRF simulations of the current and future climate of North America. NCAR Research Data Archive, Computational and Information Systems Laboratory, accessed 15 January 2018, https://doi.org/10.5065/D6V40SXP.

——, and Coauthors, 2011: High-resolution coupled climate runoff simulations of seasonal snowfall over Colorado: A process study of current and warmer climate. *J. Climate*, **24**, 3015–3048, https://doi.org/10.1175/2010JCLI3985.1.

Schär, C., C. Frei, D. Lüthi, and H. C. Davies, 1996: Surrogate climate-change scenarios for regional climate models. *Geophys. Res. Lett.*, **23**, 669–672, https://doi.org/10.1029/96GL00265.

Smith, A. B., and R. W. Katz, 2013: US billion-dollar weather and climate disasters: Data sources, trends, accuracy and biases. *Nat. Hazards*, **67**, 387–410, https://doi.org/10.1007/s11069-013-0566-5.

Swanson, K. L., 2008: Nonlocality of Atlantic tropical cyclone intensities. *Geochem. Geophys. Geosyst.*, **9**, Q04V01, https://doi.org/10.1029/2007GC001844.

Tang, B. H., and J. D. Neelin, 2004: ENSO influence on Atlantic hurricanes via tropospheric warming. *Geophys. Res. Lett.*, **31**, L24204, https://doi.org/10.1029/2004GL021072.

Thompson, G., and T. Eidhammer, 2014: A study of aerosol impacts on clouds and precipitation development in a large winter cyclone. *J. Atmos. Sci.*, **71**, 3636–3658, https://doi.org/10.1175/JAS-D-13-0305.1.

Torn, R. D., and C. Snyder, 2012: Uncertainty of tropical cyclone best-track information. *Wea. Forecasting*, **27**, 715–729, https://doi.org/10.1175/WAF-D-11-00085.1.

Walsh, K. J. E., and Coauthors, 2016: Tropical cyclones and climate change. *Wiley Interdiscip. Rev.: Climate Change*, **7**, 65–89, https://doi.org/10.1002/wcc.371.

Yates, D., B. Q. Luna, R. Rasmussen, D. Bratcher, L. Garre, F. Chen, M. Tewari, and P. Friis-Hansen, 2014: Stormy weather: Assessing climate change hazards to electric power infrastructure: a Sandy case study. *IEEE Power Energy Mag.*, **12**, 66–75, https://doi.org/10.1109/MPE.2014.2331901.